# On the Concept of Hemilability: Insights into a Donor-Functionalized Iridium(I) NHC Motif and Its Impact on Reactivity

Korbinian Riener,[†] Mario J. Bitzer,[†] Alexander Pöthig,* Andreas Raba, Mirza Cokoja, Wolfgang A. Herrmann, and Fritz E. Kühn*

Chair of Inorganic Chemistry/Molecular Catalysis, Catalysis Research Center, Technische Universität München, Ernst-Otto-Fischer-Straße 1, 85747 Garching bei München, Germany

S *Supporting Information*

ABSTRACT: Novel iridium(I) complexes bearing N-donor-functionalized N-heterocyclic carbene ligands were synthesized. Although hemilabile coordination of the attached donor is considered beneficial in catalysis, no detailed study of this phenomenon in these systems is available to date. The present report provides insight into the hemilabile bonding properties of a N,N′-bis(pyridin-2-yl)-imidazolylidene (NCN) ligand motif on iridium(I). In most cases, the presented compounds exhibit rare fluxional hemilabile coordination of the N donor, and remarkable performance in catalytic transfer hydrogenation is observed. Further, extensive reactivity studies often led to unexpected products.
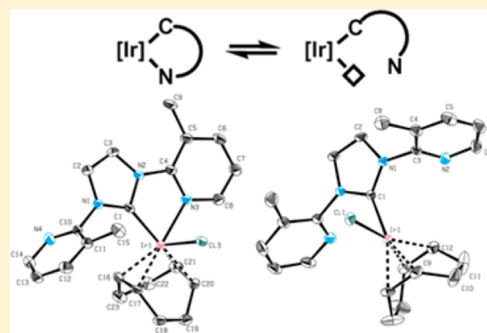
INTRODUCTION

For decades, the combination of transition metals and multidentate ligands has proven to be a viable symbiosis between interesting structural coordination chemistry and valuable catalytic applications.[1] With at least one of the donor functionalities being labile, the field of hemilabile compounds has emerged as a growing area of research (Scheme 1).[2,3]

Scheme 1. Hemilabile Coordination of a Bidentate Ligand Motif
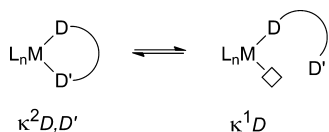
In catalytic applications, such hemilabile ligands can create vacant coordination sites, stabilize intermediate species, and precoordinate/activate the substrate, which can all enhance the catalytic performance. Among the applied systems, iridium(I) complexes bearing N-donor-functionalized N-heterocyclic carbene (NHC) ligands have been successfully employed in various catalytic transformations.[4] NHCs as neutral two-electron donors show pronounced σ-donor ability and form strong bonds to most transition metals.[5] In combination with the weaker bound N-donor function, these iridium(I) compounds were used, for example, in hydrogenation and transfer hydrogenation reactions—also in asymmetric transformations—and in hydrosilylations.[4] Although this complex motif has been widely applied in catalysis, hemilability has not yet been investigated in detail. Instead, the importance of the

hemilabile nitrogen donors was apparently more based on assumptions rather than underpinned by experimental data.

On the basis of the interest in the synthesis and application of transition metal NHC complexes and in particular their multidentate variants,[5a,6] a new iridium(I) motif coordinated by a N,N′-bis(pyridin-2-yl)-imidazolylidene (NCN) ligand is reported in this work. A novel facile and scalable route toward 1,3-bis(pyridin-2-yl)-substituted imidazolium salts and derivatives and the synthesis of the respective iridium(I) NCN complexes are presented. Most compounds could be unambiguously characterized via X-ray crystallography, and interestingly, the hemilabile character of this ligand class on iridium could be proven in the solid state by crystallization of κ^1C as well as κ^2C,N coordination of the NCN moiety. To the best of our knowledge, this is the first report on iridium(I) complexes bearing functionalized NHC ligands, which show this kind of fluxional hemilabile behavior, also presenting a quantitative measure (via density functional theory (DFT) calculations) of how weakly bound the N donor is. With regard to applications, the iridium(I) motif shows superior performance in the transfer hydrogenation of acetophenone. To get further insights into the hemilabile nature of the N donor, besides DFT calculations and variable temperature (VT) NMR experiments, reactivity studies—that is, ligand addition, halide abstraction, ligand substitution, and oxidative addition—were performed to gain a detailed understanding of the coordination modes in this complex motif.
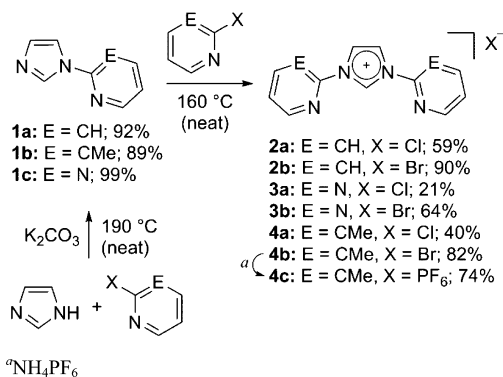
■ RESULTS AND DISCUSSION

Ligand Precursor Synthesis. 1,3-Bis(heteroaryl)-imidazolium salts **2−4** were synthesized in a two-step synthesis starting from 1*H*-imidazole (Scheme 2).

Scheme 2. Synthesis of 1-(*N*-Heteroaryl)imidazoles 1a−c and Imidazolium Salts 2−4

1a: E = CH; 92%
1b: E = CMe; 89%
1c: E = N; 99%

2a: E = CH, X = Cl; 59%
2b: E = CH, X = Br; 90%
3a: E = N, X = Cl; 21%
3b: E = N, X = Br; 64%
4a: E = CMe, X = Cl; 40%
a **4b:** E = CMe, X = Br; 82%
4c: E = CMe, X = PF₆; 74%

*a*NH₄PF₆

In the first step, which was recently developed in our group,[7] 1*H*-imidazole, 2-halo-(*N*-heterocycles), and K₂CO₃ were heated at 190 °C in sealed pressure tubes (see Supporting Information for further specifications). The obtained crude products were isolated by precipitation from methanol solution via addition of diethyl ether, giving the 1-(*N*-heteroaryl)-imidazoles **1a−c** in high yields. These compounds were further treated with small excess of the 2-halo-(*N*-heterocycle) again in sealed pressure tubes at 160 °C (or at 110 °C for **3a**), resulting in the formation of the desired imidazolium salts (**2−4a,b**) upon precipitation from methanol solution using diethyl ether. This method can be used as a facile and scalable route to a variety of 1,3-bis(pyridine-2-yl)-substituted imidazolium salts and derivatives and represents a new protocol avoiding the use of 1-methylimidazole as starting material,[8] which is so far limited to the synthesis of 1,3-bis(pyridine-2-yl)-imidazolium salts. The PF₆ derivative (**4c**) is obtained in 75% yield by exposing the respective bromide (**4b**) to an aqueous solution of ammonium hexafluorophosphate and subsequent filtration and drying of the colorless precipitate. All obtained imidazolium salts were characterized via ¹H and ¹³C NMR spectroscopy. For the nonmethylated compounds, the imidazolium NC*H*N proton resonances appear at 11.04 ppm (**2a**) and at 10.79 ppm (**2b**) in the ¹H NMR in deuterated dimethyl sulfoxide (DMSO-*d₆*); for the respective methylated derivatives (**4a−c**), the signals shift slightly upfield to ∼10.2 ppm caused by electron donation of the methyl substituents. Because of low solubility, the pyrimidyl derivatives (**3a,b**) were examined in CD₃OD, and their imidazolium NC*H*N proton resonances emerge at 10.81 and 10.45 ppm, respectively. Additionally, the novel compounds (**3** and **4**) were characterized by elemental and mass analysis, and a single crystal of **4b** suitable for X-ray diffraction could be grown by slow diffusion of diethyl ether into a solution of **4b** in acetonitrile (Figure 1).

The N1−C1 and N1−C2 bond distances with 1.334(2) Å and 1.394(2) Å, respectively, are in good accordance with the reported distances for nonmethylated salt **2a**.[8a] The same applies to the N1−C3 distance of 1.447(2) Å as well as the N1−C1−N1a angle of 108.4(2)°, while the dihedral angle C1−N1−C3−N2 is 146.2(2)°, indicating a torsion of the pyridine derivative against the planar imidazolium ring.
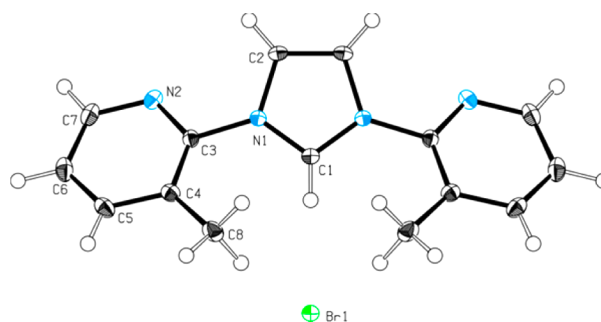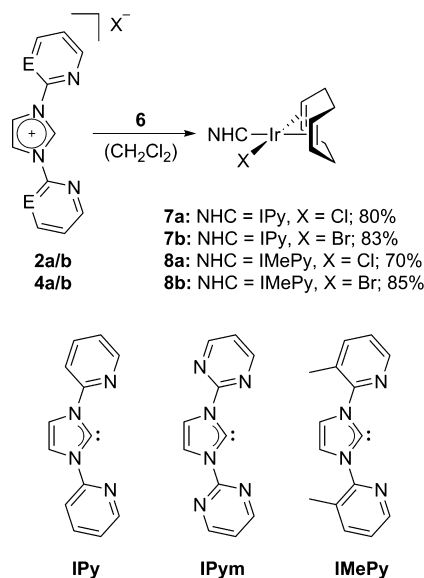
Figure 1. ORTEP-style representation of the molecular structure of **4b**. Ellipsoids are shown at the 50% probability level. Selected bond lengths (Å), angles (deg), and torsion angles (deg): C1−N1 1.334(2), C2−N1 1.394(2), C3−N1 1.447(2), C3−N2 1.326(2), C1−H1 0.90(3), Br1···H1 2.65(3), Br1···C1 3.485(2), N1−C1−N1a 108.4(2), C1−N1−C3 127.4(2), C1−H1···Br1 155.0, C1−N1−C3−N2 −146.2(2). Symmetry code: *x*, 1/2 − *y*, *z*.

Complex Synthesis and Characterization. For the synthesis of iridium(I) NHC complexes, [Ir(acac)(COD)] (**6**) was used as the metal precursor with an internal base for in situ deprotonation of the imidazolium salts. Therefore, in a modified literature procedure,[9] [IrCl(COD)]₂ (**5**) was treated with excess acetylacetone in dimethylformamide at 70 °C, yielding bright yellow [Ir(acac)(COD)] (**6**) in 72% after recrystallization from acetone.

[IrX(COD)(NHC)] complexes **7** and **8** are obtained by reaction of the respective imidazolium salts (**2a,b**, **4a,b**) and [Ir(acac)(COD)] (**6**) in dichloromethane at room temperature (Scheme 3).

The resulting compounds were precipitated by addition of *n*-pentane, filtered, and washed thoroughly with *n*-pentane. In this manner complexes [IrX(COD)(IPy)] (**7a,b**) can be obtained as red solids in ∼80% yield. Since the solubility of these compounds in chlorinated solvents is very low, NMR spectra were recorded in DMSO-*d₆*. The absence of the imidazolium

Scheme 3. Synthesis of [IrX(COD)(NHC)] Complexes 7 and 8*ᵃ*

7a: NHC = IPy, X = Cl; 80%
7b: NHC = IPy, X = Br; 83%
8a: NHC = IMePy, X = Cl; 70%
8b: NHC = IMePy, X = Br; 85%

IPy **IPym** **IMePy**

*ᵃ*Complexes with IPym could not be obtained (vide infra); abbreviations for used NHCs illustrated at the bottom.

NC*H*N proton resonance at ca. 10 ppm indicates deprotonation and carbene formation is further confirmed by a characteristic signal at ~170 ppm in the ^{13}C NMR spectrum. Only five different signals in the aromatic range of the ^{1}H NMR are present, indicating chemical equivalence of the pyridine substituents. The singlet at 8.40 ppm can be assigned to the protons of the NHC backbone; the pyridine signals range from 8.66 to 7.66 ppm, and since the spectra of **7a** and **7b** are almost equivalent, the chemical shifts seem to be independent of the coordinated halide. However, repeated measurements of the same samples indicate the formation of hydridic species as evidenced by characteristic signals at −22 ppm in the ^{1}H NMR, and the transformation is significantly faster for chloro derivative **7a** (ca. 2 h) compared to the respective bromo complex **7b** (ca. 48 h). This is in accordance with previously reported halide effects in transition metal chemistry.[10] The process is probably caused by internal C−H activation in 3-position of the pyridine moieties (see Supporting Information). The occurrence of such internal activation has been reported previously for similar systems bearing aryl-functionalized NHCs.[11] Because of low solubility in all applied solvents and insufficient stability of complexes **7a,b**, no single crystals suitable for X-ray diffraction could be obtained to clarify the coordination geometry. This gave reason to modify the ligand precursors by substitution in 3-position of the pyridines to prevent internal C−H activation. 1,3-Bis(pyrimidine-2-yl)-imidazolium salts **3a,b** were targeted as suitable ligand precursors; however, all attempts to synthesize and isolate the respective [IrX(COD)(IPym)] complexes failed. Besides variation of the solvent and reaction temperature, further iridium sources bearing internal bases such as [Ir(OMe)-(COD)]₂ or [IrCl(COD)]₂ in combination with external base or free carbene were employed but did not yield the desired product. All performed reactions resulted in complete decomposition of the applied starting materials, and no defined products could be identified by means of NMR spectroscopy. Bibliographic studies show that no iridium(I) pyrimidyl-functionalized NHC complex is known so far, suggesting an intrinsic problem in this case. Therefore, C-3-methylated imidazolium salts **4a,b** were synthesized as alternative ligand structures that should be resistant to C−H activation. The modified [IrX(COD)(IMePy)] complexes (**8a,b**) are synthesized using the same procedure as described above (Scheme 3), and the compounds are obtained as red powder in 70−85% yield. Although the solubility of these complexes in chlorinated solvents is considerably increased, DMSO-d_6 is the solvent of choice for NMR characterization to allow for better comparability to the [IrX(COD)(IPy)] complexes (**7a,b**). Chemical equivalence of the pyridyl moieties is indicated by the appearance of only four aromatic signals in the ^{1}H NMR spectra. Compared to **7a,b**, a slight upfield shift can be observed for **8a,b**, with the singlet of the NHC backbone protons now emerging at 8.29 ppm, and the pyridine signals covering the range between 8.41 and 7.58 ppm, again independent of the coordinated halide. This observation is consistent with the donating effect of the methyl groups in the modified ligand. The complexes are stable in DMSO solution, and single crystals suitable for X-ray diffraction could be obtained by slow diffusion of *n*-pentane into a dichloromethane solution of **8a,b**. Yellow and red crystals were identified for **8a**, while for **8b** only the latter was observed. All crystals were examined by means of X-ray diffraction, revealing monodentate (κ^1C) coordination in the yellow-colored species and bidentate (κ^2C,N) coordination

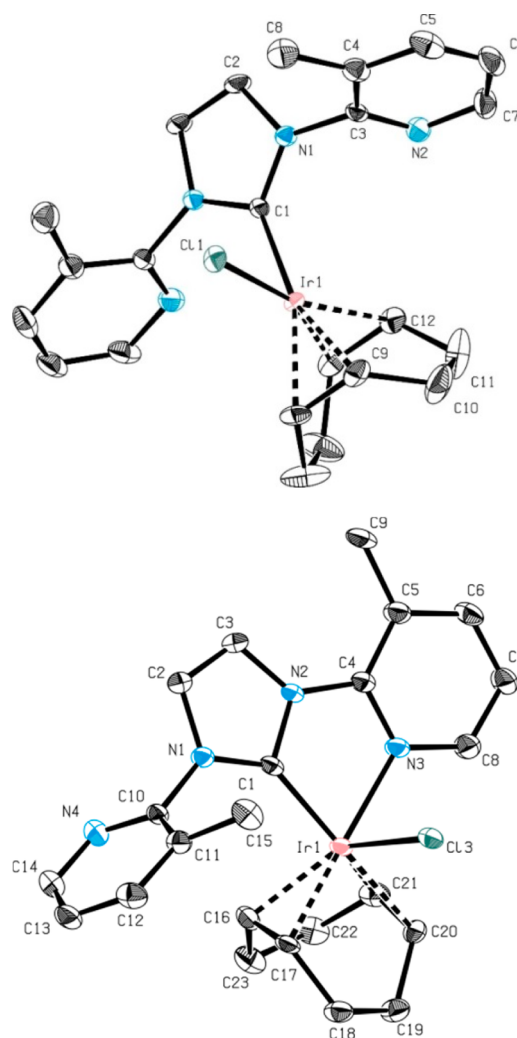in the red crystals (Figure 2 for **8a**; see Supporting Information for **8b**).

Figure 2. ORTEP-style representation of the molecular structures of κ^1C-**8a** (top) and κ^2C,N-**8a** (bottom). Hydrogen atoms as well as cocrystallized solvent molecules are omitted for clarity. Selected bond lengths (Å), angles (deg), and torsion angles (deg): κ^1C-**8a**: Ir1−Cl1 2.358(2), Ir1−C1 2.049(4), Ir1−C9 2.174(3), Ir1−C12 2.105(4), C1−Ir1−Cl1 86.9(2), N1−C1−N1a 103.6(4), C1−N1−C3−N2 72.2(4). Symmetry code: *x*, −*y* + 1/2, *z*. κ^2C,N-**8a**: Ir1−Cl3 2.5759(9), Ir1−C1 2.000(4), Ir1−N3 2.117(3), Ir1−C16 2.142(4), Ir1−C17 2.117(3), Ir1−C20 2.189(4), Ir1−C21 2.163(4), C1−Ir1−Cl3 96.31(11), C1−Ir1−N3 76.37(13), N3−Ir1−Cl3 82.28(9), C1−N2−C4−N3 5.5(5), C1−N1−C10−N4 −111.5(4).

The Ir1−C1 distance of 2.000(4) Å in the square pyramidal κ^2C,N coordination mode of **8a,b** is shorter than in square planar κ^1C-coordinated **8a** with 2.049(4) Å, but both values are comparable to iridium−carbene distances of similar pyridine-functionalized NHC complexes.[4c,d,i,12] The Ir1−N3 distance in κ^2C,N-**8a** is 2.117(3) Å. Noteworthy, the crystal structure of the κ^2C,N coordination mode contrasts with previous reports on neutral N-donor-functionalized iridium(I) carbene complexes bearing a cyclooctadiene and halide ligand, which are almost exclusively monocoordinated solely by the NHC.[4c,d,f−i,13] For the first time the occurrence of coexisting κ^1C/κ^2C,N coordination modes in these iridium(I) carbene complexes is reported. Although the κ^1C coordination mode of

8a could only be observed in the solid state, it seems likely that **8b** can also exhibit both coordination geometries. Regarding the ^{1}H NMR spectra, the appearance of two coordination geometries should result in at least two different sets of pyridine signals, but as discussed above, only four signals in the aromatic region are observed for **8a,b**. This could imply a fast equilibrium between the κ^1C and κ^2C,N coordination modes in solution as illustrated in Scheme 4, and because of similar signal sets in the ^{1}H NMR, this concept might also apply for nonmethylated species **7a,b**.

Scheme 4. Suggested Equilibrium of κ^2C,N and κ^1C Coordination
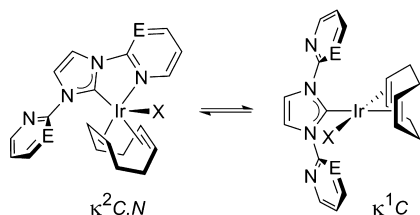
The observed fluxional behavior at room temperature clearly points out the hemilabile character of the N donor. It is a very rare phenomenon for donor-functionalized carbene complexes and is reported as either a halide- or solvent-assisted process, which seems highly unlikely in our case.[8a] To the best of our knowledge, no such fluxional iridium(I) complex bearing N-functionalized carbenes has been reported to date. Variable-temperature (VT) NMR studies were performed at low temperatures to examine this behavior in more detail. For these experiments CD$_2$Cl$_2$ was used as solvent, resulting in a slightly different appearance of the spectra compared to those recorded in DMSO-d_6. For example, the signal of the NHC backbone protons shifts from 8.29 ppm in DMSO-d_6 to 7.55 ppm in CD$_2$Cl$_2$. The samples were cooled from room temperature to −90 °C in 10 °C increments and were subsequently heated back to room temperature using the reverse temperature protocol. Detailed results of the VT NMR measurements are provided in the Supporting Information. The obtained data (selected region for **8b** shown in Figure 3) indicate that the fluxional process is considerably decelerated at −90 °C, as most of the aromatic signals vanish due to coalescence at this temperature, and coalescence of the NHC backbone protons can be observed at ca. −80 °C. A similar

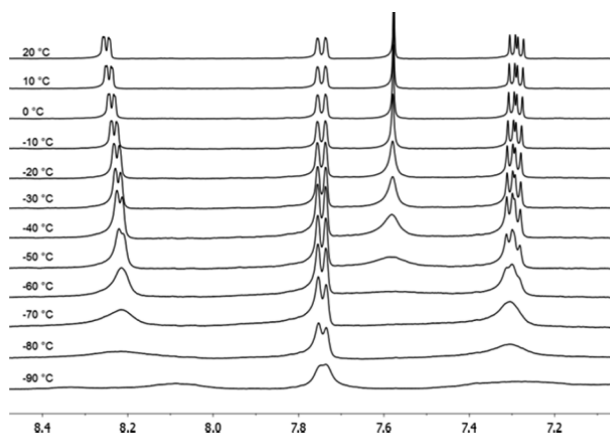behavior can be observed for the signals of the COD ligand as well as for the methyl groups in [IrX(COD)(IMePy)] complexes **8a,b**. However, separate signals for each species cannot be obtained even if cooled to the low-temperature limit of dichloromethane. This observation indicates a rapid process on the NMR time scale. Nevertheless, the data obtained from VT NMR studies supports the assumed fluxional equilibrium in solution.

Compounds **7b** and **8a,b** showed almost identical low-temperature behavior. A difference of ∼20 °C in the coalescence temperature in **8a,b** might be caused by the influence of the coordinated halide.[14] Because of insufficient stability and solubility (vide supra), no satisfying VT NMR of **7a** can be obtained.

Since the presented crystal structures as well as VT NMR experiments clearly indicate small energy differences between κ^1C and κ^2C,N coordination, an energetic quantification of this phenomenon was intended using DFT methodology. This seemed crucial to gain further insights into this fluxional process, and therefore, calculations were carried out to obtain an energy profile along the κ^1C (**GS_1**)/κ^2C,N (**GS_2**) coordination including the respective transition state (**TS**) as illustrated in Figure 4.
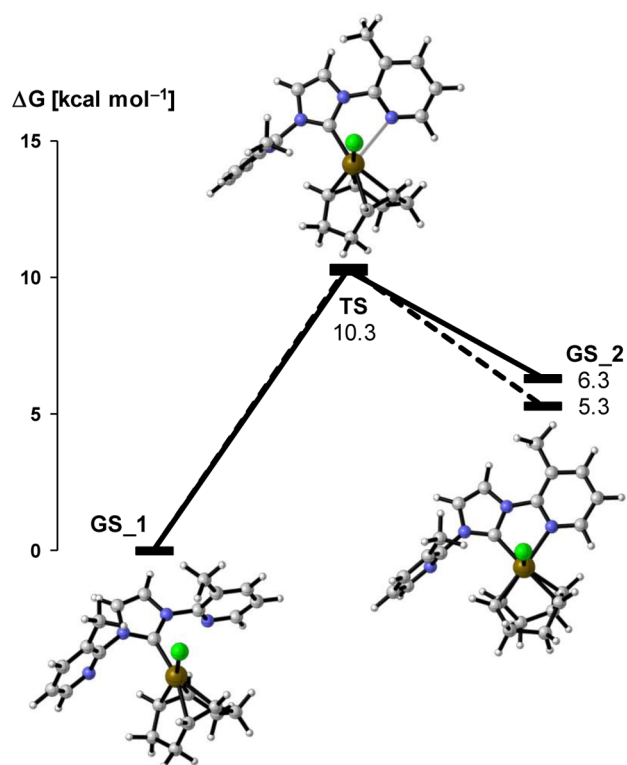

Figure 4. Free energy profile (B3LYP/6-31+G**) along the κ^1C/κ^2C,N coordination in [IrX(COD)(IMePy)] **8a,b** (black line for chloro complex **8a** (also optimized geometries shown), dashed line for bromo complex **8b**).

In both the chloro and bromo complexes **8a,b**, the square planar κ^1C ground states (**GS_1**) show slightly higher stability than the square pyramidal κ^2C,N ground states (**GS_2**) by 5 and 6 kcal/mol, respectively. Additionally, the small energy barriers for the N-coordination of 10 kcal/mol for both the chloro and bromo complex are in good accordance with the observed fluxional behavior in solution. The barriers for the

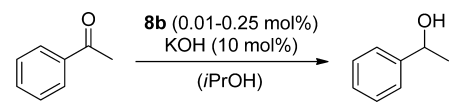**Figure 3.** VT NMR study of **8b** in CD$_2$Cl$_2$ (selected region).

decoordination, the reverse reaction, from ground states **GS_2** to **GS_1** are 4 kcal/mol (chloro complex **8a**) and 5 kcal/mol (bromo complex **8b**). These results support the existence of a possible equilibrium between the $\kappa^1 C$ and $\kappa^2 C,N$ coordination.

When looking into literature on hemilabile ligand systems, one would also consider other mechanistic explanations for the observed fluxional processes.[2] Besides the $\kappa^1 - \kappa^2$ mechanism proposed in this work, which is based on the observed crystal structures, VT-NMR data, and DFT calculations, further possibilities need to be mentioned. When looking at a $\kappa^2 - \kappa^2$ process, there are two possible mechanisms, namely, associative and dissociative. However, with regard to sterics, these seem to be quite challenging since the NCN ligand would have to coordinate in a tridentate fashion for the associative mechanism, and also a concerted displacement of the pyridine in a dissociative mechanism seems to be sterically constrained. To the best our knowledge, there is no report on this ligand motif that unambiguously verifies a tridentate, pincer-type coordination to a single metal center. Further, conformational changes could also be involved. Although a $\kappa^1 - \kappa^2$ fluxional process is still assumed as the most plausible mechanism in this work, all above-described processes need to be mentioned to provide a broader scope of potential contributions to the observed phenomena.

Transfer Hydrogenation Catalysis. Since iridium(I) complexes bearing NHC ligands have been widely applied in catalysis,[4h,i,5f,15] the impact of fluxional hemilability on the catalytic performance is of great interest. In this context, catalytic transfer hydrogenation is one of the most important applications.[4h,i,15a−n] Because of its stability, solubility, and high-yielding synthesis, **8b** was employed in the reduction of acetophenone with isopropanol as hydrogen donor and KOH as base to get insight into the potential beneficial properties of the fluxional hemilabile behavior. As illustrated in Table 1, **8b** appears to be a highly suitable candidate for this type of reaction since loadings as low as 0.01 mol % proved to efficiently catalyze the hydrogen transfer.

The obtained results point toward exceptional catalytic performance of **8b** as turnovers reach 9000 at 0.01 mol % catalyst loading, which also shows the robustness of the system at such low catalyst concentrations. To the best of our knowledge, this is the highest value of any reported iridium(I) NHC compound in the catalytic transfer hydrogenation of

acetophenone to date. Therefore, it seems that donor functionalization can lead to stabilization of the catalyst resulting in increased catalytic turnovers. With regard to the activity, the turnover frequency given at 50% conversion (TOF_{50}) of 7500 h^{-1} is as well among the highest published figures, and only three articles reported higher values.[4h,15m,n] Merely one catalyst system—bearing a nondonor-functionalized benzimidazolylidene-derived ligand with bulky substituents—shows a significantly higher activity (by a factor of 5),[15m] and all others are within the same order of magnitude as the catalyst activities reported here.[4h,15n] In donor-functionalized systems, work by Jiménez and Pérez-Torrente et al.[3i] shows that O-donor-functionalized NHC ligands on iridium(I) lead to better catalytic activity than its N-analogues, which might suggest that a strongly donating functionality on the NHC moiety could potentially reduce its activity. However, the discussion of such a trend would be quite speculative based on the values obtained in this study, since the catalytic activity of the systems is still comparably high.

Reactivity Studies. To further systematically investigate and understand the coordination phenomenon of fluxional hemilability in the Ir NCN motif, detailed reactivity studies were carried out, that is, ligand addition, anion variation, ligand substitution as well as oxidative addition. These reactions seemed interesting to reveal the properties of the fluxional hemilabile bond and to see if N bonding can be strengthened or even prevented in the obtained compounds. To clearly illustrate if the pyridine moiety shows fluxional hemilabile coordination, a dashed line is used from now on to define these bonds in the respective complexes (see Figure 5).
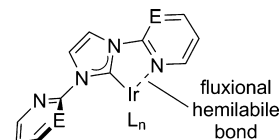
Figure 5. Used convention to illustrate fluxional hemilability in a given complex.

With respect to the planned reactivity studies, the expected reaction products are illustrated in Figure 6. As for the catalytic evaluation, complex **8b** was again chosen as starting material for all reactivity studies due to its stability, solubility, and high-yielding synthesis.

Regarding phosphine addition (**I**), it was expected that the addition of a phosphine would permanently displace the labile pyridine moiety, similar to what was observed for a related palladium complex bearing a structurally closely related NHC motif.[8a] The resulting iridium(I) complex would then be coordinated by a COD, a halide as well as an NHC and phosphine ligand. Although no such structures have been reported for Ir(I) to date, analogous structures with two phosphines in a square pyramidal coordination geometry are known.[17] Therefore, it seemed reasonable to assume a structure with a nonfluxional $\kappa^1 C$ coordination of the NCN ligand as shown in Figure 6. For halide abstraction (**II**), a square planar geometry with $\kappa^2 C,N$ coordination of the NCN motif was expected.[12] In the reactivity toward carbon monoxide (**III**), iridium(I) compounds with an NHC, two CO, and a halide ligand are reported as square planar complexes.[15m,18] This also applies to N-donor-functionalized NHC ligands, which would again lead to $\kappa^1 C$ coordination of the NCN moiety as in the

Table 1. Catalytic Hydrogen Transfer from 2-Propanol to Acetophenone Using 8b[a]

entry	catalyst[b] [mol %]	yield[c] [%]	TOF_{50}[d] [h^{-1}]	turnovers[e]
1	0.25	99	1200	400
2	0.10	95	2300	950
3	0.05	90	2600	1800
4	0.01	90	7500	9000

[a]Reaction conditions: acetophenone (5 mmol), KOH (0.5 mmol, 10 mol %), iPrOH (6.5 mL), 82 °C, 240 min. [b]As already reported in literature,[16] product formation was also observed without catalyst (24% yield). [c]Yields determined via ^{1}H NMR using mesitylene as internal standard. [d]Turnover frequency (TOF) given at 50% conversion (TOF_{50}). [e]Turnovers are defined as [1-phenylethanol]/[**8b**] (for a single catalysis run).
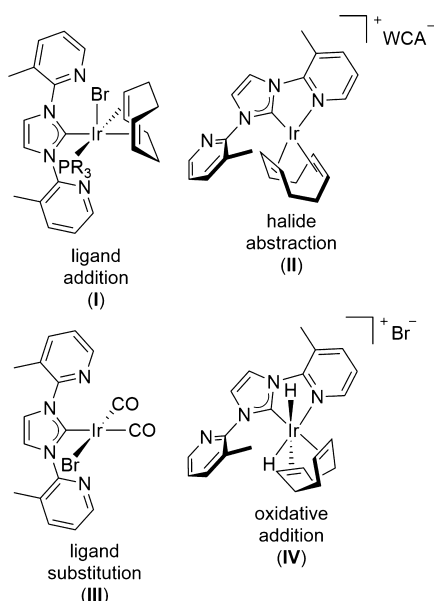
Figure 6. Expected structures in the reactivity studies (WCA = weakly coordinating anion).

case of **I**.[4h] Finally, oxidative addition (**IV**) of dihydrogen should result in κ^2C,N coordination of the NCN ligand in an octahedral coordination geometry.[19]

In a first experiment **8b** was treated with 1 equiv of trimethylphosphine at room temperature, and an immediate color change from dark red to orange could be observed. After solvent evaporation and washing with *n*-pentane, the phosphinated yellow complex [Ir(COD)(IMePy)(PMe$_3$)]Br (**9a**) is obtained in 75% yield (Scheme 5). The ^{1}H NMR

Scheme 5. Synthesis of Cationic Phosphine Complexes 9a,b
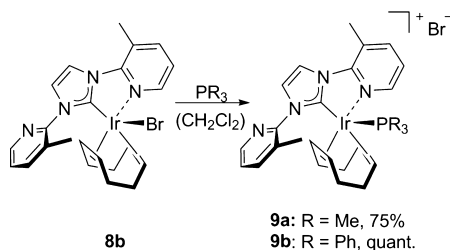

spectrum of **9a** again exhibits four aromatic signals, indicating a symmetric coordination geometry. The signal of the NHC backbone protons emerges at 8.24 ppm, and the pyridine protons cover the range from 8.17 to 7.43 ppm, which is a slight upfield shift compared to the pyridine proton signals in **8a,b**. A doublet at 1.16 ppm indicates the coordination of 1 equiv of PMe$_3$, which is also confirmed by a signal at −42.8 ppm in the ^{31}P NMR. Accordingly, the carbene signal in the ^{13}C NMR at 172.0 ppm appears as a doublet with a $^2J_{CP}$ coupling constant of 7.2 Hz. To elucidate possible hemilability, VT NMR studies of **9a** were performed, and the obtained results indicate fluxional behavior as observed for compounds **7** and **8** (see Supporting Information). In various attempts, no single crystals suitable for X-ray diffraction experiment could be obtained. However, the results of the VT NMR give reason to postulate the cationic structure of **9a** as depicted in Scheme 5. This therefore implies an unexpected reactivity of **8b**, as the phosphine rather substitutes the bromide instead of displacing

the pyridine. A possible explanation might be that the resulting compound bearing a carbene as well as a phosphine and a halide might be too electron-rich; thus, the coordinated halide is converted to an outer-sphere anion. The assumed geometry is underpinned by the crystal structure of the WCA-bearing cationic derivative **10** (vide infra), which exhibits an identical ^{1}H NMR spectrum as that of **9a**.

To study steric effects on the observed reactivity, the sterically more demanding triphenylphosphine was applied as reactant,[20] and similar results were obtained (Scheme 5, also see Supporting Information), supporting the assumption that the displacement of the coordinated halide might be of electronic origin. Again, an immediate color change was observed upon exposition at room temperature, and after solvent evaporation and washing with *n*-pentane, [Ir(COD)-(IMePy)(PPh$_3$)]Br (**9b**) was obtained as yellow powder in quantitative yield. The ^{1}H NMR of **9b** exhibits an upfield-shifted signal of the NHC backbone protons at 7.96 ppm (compared to 8.24 ppm for **9a**), and the pyridine proton signals cover the range from 8.27 to 7.55 ppm (8.17−7.43 ppm in case of **9a**). The signal of the proton in 6-position of the pyridines at 8.27 ppm appears as a very broad singlet, while all other signals display the expected multiplicities. The inclusion of 1 equiv of PPh$_3$ is proven by the presence of three aromatic signals at 7.43, 7.33, and 7.10 ppm with an integral ratio of 3:6:6 and the respective signal in the ^{31}P NMR at −3.1 ppm. The carbene signal in the ^{13}C NMR appears as a doublet at 170.8 ppm with a $^2J_{CP}$ coupling constant of 10.5 Hz. As in case of **9a**, fluxional behavior can also be observed in **9b** by the appearance of the respective VT NMR spectra (see Supporting Information).

For further characterization of the coordinative properties the synthesis of derivatives of complexes **7** and **8** bearing weakly coordinating anions was attempted. In a first experiment, the attempt was made to abstract the coordinated halide of **8a,b** with common reagents such as AgPF$_6$, KPF$_6$, NH$_4$PF$_6$, and NaBF$_4$, but all experiments either resulted in complete decomposition (AgPF$_6$) or no reaction was observed. In a second attempt, the PF$_6$ imidazolium salt (**4c**) was used under identical conditions as applied for the synthesis of **8a,b** (Scheme 3). Although in situ NMR experiments in DMSO-d_6 solution indicate product formation (see Supporting Information), all attempts to isolate a defined product failed, and in most cases only the imidazolium salt could be reisolated. Possibly the weak interaction between the metal center and the pyridine moiety cannot stabilize the resulting complex sufficiently to be isolated upon halide abstraction. However, since the desired complex is formed in situ, the presence of coordinating solvent in the reaction mixture might enable product formation. This resulted in modification of the reaction protocol by adding stabilizing donors like acetonitrile or trimethylphosphine. Unfortunately, no product formation was observed using the former reagent, but reacting PF$_6$ imidazolium salt **4c** with [Ir(acac)(COD)] (**6**) in the presence of 1 equiv of trimethylphosphine in dichloromethane yields [Ir(COD)(IMePy)(PMe$_3$)](PF$_6$) (**10**) as a yellow solid (Scheme 6).

The ^{1}H NMR spectrum of **10** is identical to the respective spectrum of **9a** suggesting the same fluxional behavior, and apart from the PF$_6$ septet of **10** at −144.2 ppm, this also applies to the ^{31}P NMR spectrum. The $^2J_{CP}$ coupling constant of the carbene at 172.0 ppm in the ^{13}C NMR spectrum is 6.9 Hz. However, the product was always accompanied by a side product. Judging from the ^{1}H and ^{31}P NMR spectra (see

Scheme 6. Synthesis of 10 from Imidazolium Salt 4c
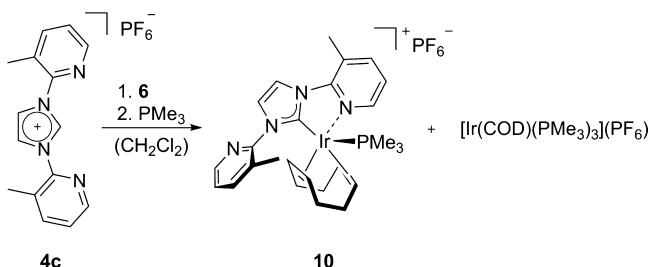
Supporting Information), this side product could be identified as $[Ir(COD)(PMe_3)_3](PF_6)$, which is known to form in similar reactions.[21]

As an alternative route to **10**, compound **9a** was chosen as starting material. In contrast to neutral compound **8b** bearing a coordinated halide, cationic **9a** allows for clean exchange of the anion using NH_4PF_6 without formation of any side product, yielding **10** as an orange solid in 90% yield (Scheme 7).

Scheme 7. Synthesis of 10 via Anion Exchange
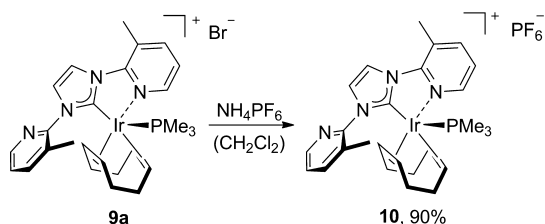
Crystals suitable for X-ray crystallography were obtained by slow diffusion of *n*-pentane into a solution of **10** in dichloromethane (Figure 7). The compound crystallizes in
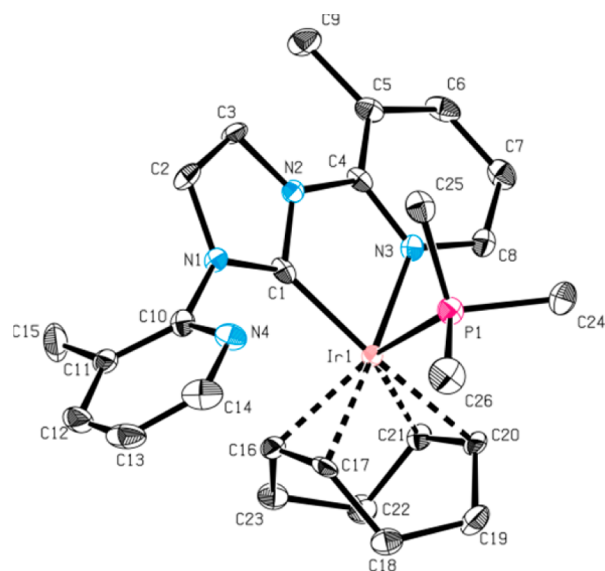

Figure 7. ORTEP-style representation of the molecular structure of **10**. Ellipsoids are shown at the 50% probability level. Hydrogen atoms as well as the PF_6-anion are omitted for clarity. Selected bond lengths (Å), angles (deg), and torsion angles (deg): Ir1−P1 2.359(1), Ir1−C1 1.984(4), Ir1−N3 2.119(3), Ir1−C16 2.147(4), Ir1−C17 2.122(4), Ir1−C20 2.196(4), Ir1−C21 2.184(4), C1−Ir1−P1 90.17(11), C1−Ir1−N3 76.72(13), N3−Ir1−P1 90.58(9), C1−N2−C4−N3 −8.1(5), C1−N1−C10−N4 72.9(5).

square pyramidal geometry with κ^2C,N coordination of the NCN ligand, while no crystals exhibiting monodentate coordination could be obtained. Because of the similarity in the ^1H NMR spectra, the same molecular structure can be assumed for **9a,b**. This result is in accordance with related cationic compounds bearing COD and N-donor-functionalized carbene ligands,[4a,b,d,f,g,i,j,22] proving that the interaction between the metal center and the pyridine moiety is not considerably increased even in a cationic species.

The Ir1−C1 bond length is 1.984(4) Å and is therefore only slightly shorter than in the case of κ^2C,N-**8a** (2.000(4) Å). The Ir1−N3 distance of 2.119(3) Å is almost identical to that of **8a** (2.117(3) Å), and the distance between the iridium center and the phosphorus atom (Ir1−P1) is 2.359(1) Å. This is similar to the respective bond length in iridium(I) complexes bearing monodentate NHC ligands.[23]

To study ligand substitution, compound **8b** was treated with CO: A dark red dichloromethane solution of **8b** was exposed to 1 bar of carbon monoxide at room temperature, and the color immediately changed to intense purple. When the solution was purged with argon it became bright red. This phenomenon is reversible if the solution was again exposed to CO. After evaporation of the solvent and washing with pentane, the carbonyl complex $[IrBr(CO)(IMePy)]$ (**11**) is obtained as bright red powder in quantitative yield (Scheme 8). The ^1H

Scheme 8. Synthesis of 11 via Ligand Substitution
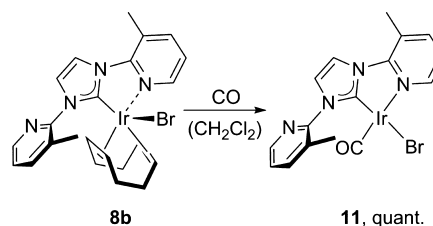
NMR displays two signals of the NHC backbone protons at 7.93 and 7.01 ppm and six pyridine proton signals ranging from 9.69 to 7.37 ppm as well as two methyl group signals at 2.76 and 2.32 ppm. This suggests a nonfluxional κ^2C,N coordination geometry of the NCN ligand, which is confirmed by VT NMR experiments revealing no alteration of the spectra at lower temperatures. In the ^{13}C NMR, the carbene C is found at 177.0 ppm, and only one carbonyl signal appears at 170.7 ppm. Single crystals suitable for X-ray diffraction were grown by slow diffusion of *n*-pentane into a dichloromethane solution of **11**, and the obtained crystal structure unveils a monocarbonyl iridium complex, which contrasts the expected and reported reactivity with related compounds exclusively bearing two CO ligands,[15m,18] also for N-donor-functionalized NHCs (Figure 8).[4h] Therefore, **11** represents the first monocarbonyl iridium NHC compound obtained by direct exposure of carbon monoxide to a $[IrX(COD)(NHC)]$ complex. As in case of ligand addition, the unusual coordination behavior of the presented NCN ligand once again leads to an unexpected reaction outcome.

Regarding the crystal structure of **11**, the carbonyl ligand is orientated trans to the pyridine with the bromide coordinated trans to the carbene. The C1−Ir1 bond length of 1.921(4) Å is significantly shorter than in the COD-bearing derivatives (**8a,b**), and the bond length between Ir1 and N3 of 2.109(4) Å is very similar to **8b** (2.117(3) Å). The Ir−CO distance is 1.806(6) Å. In solid-state IR measurements, the CO stretching
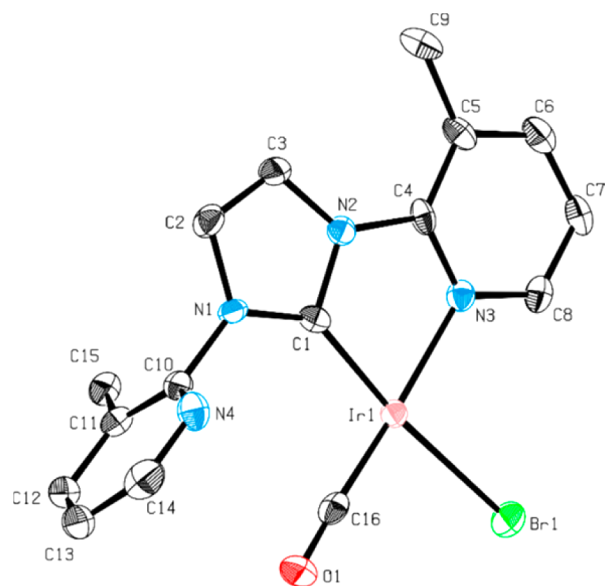
Figure 8. ORTEP-style representation of the molecular structure of **11**. Ellipsoids are shown at the 50% probability level. Hydrogen atoms as well as the PF_6 anion are omitted for clarity. Selected bond lengths (Å), angles (deg), and torsion angles (deg): Ir1–Br1 2.35049(11), Ir1–C1 1.921(4), Ir1–N3 2.109(4), Ir1–C16 1.806(6), C1–Ir1–Br1 171.7(2), C1–Ir1–N3 77.2(2), C16–Ir1–N3 174.3(2), N3–Ir1–Br1 94.7(2), C1–N2–C4–N3 0.2(6), C1–N1–C10–N4 89.8(6).

band is found at 1960 cm^{-1} indicating significant weakening of the carbon–oxygen triple bond.[24] Further experiments focused on the origin of the purple color of the reaction solution under CO atmosphere. Therefore, an NMR sample of the purple intermediate in CD_2Cl_2 under CO atmosphere (3 bar) was measured, but the resulting proton spectrum exhibits mostly broad and undefined signals (see Supporting Information). The only sharp signals are two singlets at 5.54 and 2.33 ppm, corresponding to free cyclooctadiene. The same applies to the ^{13}C NMR spectrum, where no signals apart from free cyclooctadiene can be found. However, removing the solvent from the NMR tube in vacuo yields bright red **11**. Because of the undefined signals in the NMR spectra, it is to be suspected that the purple intermediate comprises a mixture of different bridged and nonbridged multicarbonyl Ir species.

Finally, as iridium has been applied in a variety of catalytic (transfer) hydrogenation reactions,[15o] it seemed interesting to study the behavior of **8b** toward dihydrogen. Only a small number of Ir–carbene hydride complexes has been accessed by direct treatment with H_2, and hydrogenation of the coordinated olefin is common.[19,25] In a gas-sealed NMR tube, compound **8b** in CD_2Cl_2 was charged with 1 bar of dihydrogen at −78 °C. The solution instantaneously changed color from dark red to light brown. An immediate ^1H NMR spectrum of the sample was recorded at −30 °C and displays two hydride signals at −12.00 and −16.70 ppm, indicating the formation of the dihydride $[Ir(H)_2(COD)(IMePy)]Br$ (**12**) in quantitative NMR yield (Scheme 9). In the aromatic region two separate NHC backbone signals are visible at 8.24 and 7.40 ppm. The six pyridine signals are distributed in the range of 8.89−7.49 ppm. Therefore, a nonfluxional κ^2C,N coordination can be assumed for the dihydride complex, which is in accordance with the observation that N-donor-functionalized Ir(III) complexes tend to favor κ^2C,N coordination.[26] No characteristic singlet for cyclooctane as the hydrogenation product at 1.50 ppm is

Scheme 9. Formation of Dihydride Complex 12 and 2D NOESY Spectrum (Selected Region)
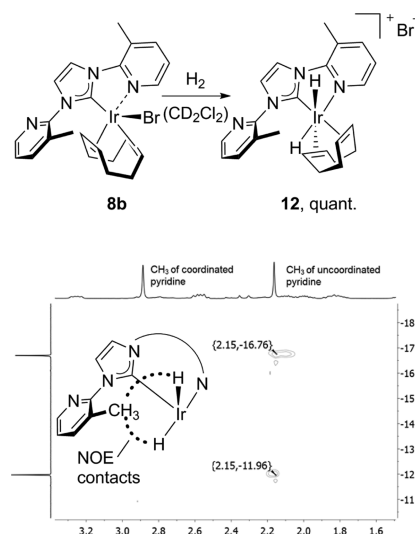
visible, but rather a set of 10 separate signals appear, accounting for 12 protons of the coordinated cyclooctadiene, with the olefinic protons as two signals at 5.02 and 4.84 ppm. The compound can be stored for days at −30 °C in CD_2Cl_2; however, if the sample is warmed to room temperature for more than 1 h, cyclooctane is formed as evidenced by the formation of the respective singlet at 1.50 ppm in the ^1H NMR. In HMQC NMR experiments, all proton signals can be assigned to their respective carbon signals in the ^{13}C NMR spectrum. Further, low-temperature NOESY experiments at −30 °C suggest a cis arrangement of the NHC and both hydride ligands in an octahedral coordination geometry since both hydrides exhibit NOE contacts to the methyl group of the noncoordinated pyridine moiety (Scheme 9; also see Supporting Information).

■ CONCLUSION

The synthesis, characterization, and reactivity of novel iridium(I) NCN complexes and a new access route to a variety of N-functionalized N-heterocyclic carbene precursors are reported. Detailed characterization via NMR spectroscopy, X-ray crystallography, and DFT calculations has revealed rare fluxional hemilability of the NCN motif including crystal structures of κ^1C as well as κ^2C,N coordination in one compound, which is a phenomenon not yet known for these systems. This type of hemilabile behavior, which has not been studied or seen in other iridium(I) NHC complexes, could not even be completely stopped at −90 °C. A computational analysis is consistent with small energy differences between the two coordination modes. These results illustrate that the attached donor functionalities should not just be depicted as coordinated or noncoordinated to the metal center, but the coordination should rather be seen as a dynamic process. In catalytic transfer hydrogenation, the obtained iridium(I) motif reaches remarkable turnovers and shows excellent activity (TOF) in the reduction of acetophenone even at low loadings, exceeding the activity and stability of comparable nonhemilabile systems. Reactivity studies—that is, ligand addition, halide abstraction, ligand substitution and oxidative addition—have shown the formation of some unexpected compounds with regard to ligand coordination as compared to similar complexes

Table 2. Crystallographic Data for 4b, κ^1C-8a, κ^2C,N-8a, 8b, 10, and 11

	4b	κ^1C-8a	κ^2C,N-8a	10	11
formula	$C_{15}H_{15}BrN_4$	$C_{23}H_{26}ClIrN_4$	$C_{24}H_{28}Cl_3IrN_4$	$C_{26}H_{35}F_6IrN_4P_2$	$C_{16}H_{14}BrIrN_4O$
fw	331.21	586.15	671.05	771.72	550.42
color/habit	clear light orange-brown fragment	clear yellow block	clear intense red fragment	clear intense yellow plate	clear intense red fragment
crystal dimens [mm³]	0.174 × 0.341 × 0.419	0.180 × 0.210 × 0.290	0.110 × 0.160 × 0.200	0.010 × 0.130 × 0.140	0.040 × 0.060 × 0.120
crystal system	monoclinic	orthorhombic	triclinic	triclinic	monoclinic
space group	$P2_1/m$ (No. 11)	$Pnma$ (No. 62)	$P\bar{1}$; (No. 2)	$P\bar{1}$; (No. 2)	$P2_1/n$
a [Å]	6.9949(2)	8.2209(2)	8.6800(5)	9.5594(3)	9.592(4)
b [Å]	14.8441(5)	17.1689(4)	9.1793(5)	12.1179(4)	14.314(7)
c [Å]	7.0265(2)	14.8962(3)	15.1898(8)	12.6163(4)	11.984(6)
α [deg]	90	90	88.714(3)	105.252(2)	90
β [deg]	100.702(1)	90	86.095(3)	94.272(1)	104.68(2)
γ [deg]	90	90	87.195(3)	95.896(1)	90
V [Å³]	716.89(4)	2102.51(8)	3031.43(16)	1394.67(8)	1591.7(13)
Z	2	4	2	2	4
T [K]	123	123	123	123	123
D_{calc} [g cm⁻³]	1.534	1.561	1.848	1.838	2.297
μ [mm⁻¹]	2.862	6.495	5.889	4.966	10.908
$F(000)$	336	1144	656	760	1032
Θ range [deg]	2.74–25.38	1.81–25.42	1.34–25.58	2.07–25.42	2.26–25.59
index ranges (h, k, l)	±8, ± 17, ± 8	±9, ± 20, ± 17	±10, ± 11, ± 18	±11, ± 14, ± 15	−11–10, ± 17, ± 14
no. of reflns collected	23 396	74 985	28 873	38 680	19 493
no. of indep reflns/R_{int}	1366	2001	4377	5137	2949
no. of obsd reflns $(I > 2\sigma(I))$	1332	1782	4113	4398	2214
no. of data/restraint/param	1366/0/125	2001/0/137	4377/0/291	5137/15/412	2949/0/210
R1/wR2 $(I > 2\sigma(I))$	0.0171/0.0422	0.0219/0.0569	0.0232/0.0534	0.0278/0.0453	0.0245/0.0364
R1/wR2 (all data)	0.0178/0.0426	0.0264/0.0583	0.0262/0.0549	0.0410/0.0480	0.0476/0.0417
GOF (on F^2)	1.082	1.077	1.081	1.017	0.998
largest diff peak/hole [e Å⁻³]	0.325/−0.207	1.013/−2.143	1.815/−1.183	0.622/−0.641	1.042/−1.067

reported in literature. Again, fluxional hemilabile behavior has been observed. The obtained results might also point toward the existence of similar dynamic behavior in more systems with a multidentate ligand motif, and accordingly, this should be seen as an incentive to study and more thoroughly understand this phenomenon. On the basis of these findings, systematic variations of the ligand motif and detailed catalytic studies are currently ongoing in our laboratories.

■ EXPERIMENTAL SECTION

General Considerations. Unless otherwise specified, all reactions were performed under oxygen-free, dry conditions in an argon atmosphere using standard Schlenk and glovebox techniques. The used solvents were purified, degassed, and dried according to standard purification techniques[27] or obtained from an M. Braun SPS purification system. If not noted differently, all further chemicals were purchased from commercial sources and were used as received. NMR spectra were acquired on a Bruker Avance Ultrashield 400 MHz and a Bruker DPX 400 MHz spectrometer. Fast-atom bombardment mass spectrometry was carried out using a Finnigan MAT 90, and electrosprary ionization mass spectra were acquired on a Thermo Scientific LCG Fleet. CHN analyses were carried out in the microanalytical laboratory at Technische Universität München. IR spectra were recorded on a Varian FTIR-670 spectrometer using a GladiATR accessory with a diamond attenuated total reflectance element. Analytical data of all obtained compounds and experimental details on the synthesis of ligand precursors, iridium(I) NHC complexes, and for catalytic transfer hydrogenation are provided in the Supporting Information.

X-ray Crystallography. Single crystals were measured in the SC-XRD laboratory of the Catalysis Research Center at Technische Universität München. Additional crystallographic information is available in the Supporting Information. Crystallographic data are further provided in Table 2 as well as in the Supporting Information.

Computational Methods. All calculations used DFT methodology as implemented in Gaussian09[28] using the density functional hybrid model B3LYP[29] and 6-31+G** as the basis set for nonmetals,[30] while the Stuttgart RSC 1997 ECP basis set was employed for Ir.[31] No symmetry or internal coordinate constraints were applied during optimizations. Calculated structures were verified as being true minima by the absence of negative eigenvalues in the vibrational frequency analysis or as transition states by presence of one and only one negative eigenvalue along the corresponding reaction coordinate in the vibrational frequency analysis. Solvent effects were simulated with the PCM model[32] as implemented in Gaussian 09, and the solvent of choice was dichloromethane. Detailed computational data is provided in the Supporting Information.

■ ASSOCIATED CONTENT

ⓈSupporting Information
Experimental procedures, NMR spectra, VT NMR data, two-dimensional (2D) NMR experiments, and crystallographic and computational details. This material is available free of charge via the Internet at http://pubs.acs.org. Crystallographic data (excluding structure factors) for the structures reported in this paper were deposited with the Cambridge Crystallographic Data Centre as supplementary publication Nos. CCDC 989706 (**4b**) and CCDC 989707 (κ^1C-**8a**), CCDC 989708 (κ^2C,N-**8a**), CCDC 989709 (**8b**), CCDC 989710 (**10**), and CCDC 989711

(11). These data can be obtained free of charge via www.ccdc. cam.ac.uk/data_request/cif.

■ AUTHOR INFORMATION

Corresponding Authors
*E-mail: alexander.poethig@tum.de. (A.P.)
*E-mail: fritz.kuehn@ch.tum.de. (F.E.K.)

Author Contributions
[†]These authors contributed equally to this work.

Notes
The authors declare no competing financial interest.

■ REFERENCES

(1) (a) Hartwig, J. F. In *Organotransition Metal Chemistry: From Bonding to Catalysis;* University Science Books: Mill Valley, CA, 2010. (b) Crabtree, R. H. In *The Organometallic Chemistry of the Transition Metals;* Wiley: Hoboken, NJ, 2011.

(2) Reviews on hemilability: (a) Bader, A.; Lindner, E. *Coord. Chem. Rev.* **1991**, *108*, 27−110. (b) Braunstein, P.; Naud, F. *Angew. Chem., Int. Ed.* **2001**, *40*, 680−699. (c) Heard, P. J. *Chem. Soc. Rev.* **2007**, *36*, 551−569. (d) Weng, Z.; Teo, S.; Hor, T. S. A. *Acc. Chem. Res.* **2007**, *40*, 676−684. (e) van der Vlugt, J. I. *Eur. J. Inorg. Chem.* **2012**, 363−375. (f) Annibale, V. T.; Song, D. *RSC Adv.* **2013**, *3*, 11432−11449. (g) Oestreich, M. *Angew. Chem., Int. Ed.* **2014**, *53*, 2282−2285.

(3) Selected examples on hemilabile systems: (a) Huynh, H. V.; Yeo, C. H.; Tan, G. K. *Chem. Commun.* **2006**, 3833−3835. (b) Zanardi, A.; Peris, E.; Mata, J. A. *New J. Chem.* **2008**, *32*, 120−126. (c) Huynh, H. V.; Yeo, C. H.; Chew, Y. X. *Organometallics* **2010**, *29*, 1479−1486. (d) Barry, B. M.; Stein, B. W.; Larsen, C. A.; Wirtz, M. N.; Geiger, W. E.; Waterman, R.; Kemp, R. A. *Inorg. Chem.* **2013**, *52*, 9875−9884. (e) Bernhammer, J. C.; Huynh, H. V. *Organometallics* **2013**, *33*, 172−180. (f) Choi, G.; Tsurugi, H.; Mashima, K. *J. Am. Chem. Soc.* **2013**, *135*, 13149−13161. (g) DePasquale, J.; Kumar, M.; Zeller, M.; Papish, E. T. *Organometallics* **2013**, *32*, 966−979. (h) Du, W.; Wu, P.; Wang, Q.; Yu, Z. *Organometallics* **2013**, *32*, 3083−3090. (i) Jiménez, M. V.; Bartolomé, M. I.; Pérez-Torrente, J. J.; Goméz, D.; Modrego, F. J.; Oro, L. A. *ChemCatChem* **2013**, *5*, 263−276. (j) Kennedy, R. D.; Machan, C. W.; McGuirk, C. M.; Rosen, M. S.; Stern, C. L.; Sarjeant, A. A.; Mirkin, C. A. *Inorg. Chem.* **2013**, *52*, 5876−5888. (k) Kennedy, R. D.; Stern, C. L.; Mirkin, C. A. *Inorg. Chem.* **2013**, *52*, 14064−14071. (l) Lee, W.-C.; Sears, J. M.; Enow, R. A.; Eads, K.; Krogstad, D. A.; Frost, B. J. *Inorg. Chem.* **2013**, *52*, 1737−1746. (m) Lifschitz, A. M.; Shade, C. M.; Spokoyny, A. M.; Mendez-Arroyo, J.; Stern, C. L.; Sarjeant, A. A.; Mirkin, C. A. *Inorg. Chem.* **2013**, *52*, 5484−5492. (n) Park, J. S.; Lifschitz, A. M.; Young, R. M.; Mendez-Arroyo, J.; Wasielewski, M. R.; Stern, C. L.; Mirkin, C. A. *J. Am. Chem. Soc.* **2013**, *135*, 16988−16996. (o) Rosen, M. S.; Stern, C. L.; Mirkin, C. A. *Chem. Sci.* **2013**, *4*, 4193−4198. (p) Specht, Z. G.; Grotjahn, D. B.; Moore, C. E.; Rheingold, A. L. *Organometallics* **2013**, *32*, 6400−6409. (q) Wang, T.; Pranckevicius, C.; Lund, C. L.; Sgro, M. J.; Stephan, D. W. *Organometallics* **2013**, *32*, 2168−2177. (r) Barrett, B. J.; Iluc, V. M. *Inorg. Chem.* **2014**, *53*, 7248−7259. (s) Biswas, S.; Zhang, A. B.; Raya, B.; RajanBabu, T. V. *Adv. Synth. Catal.* **2014**, *356*, 2281−2292. (t) Bubrin, M.; Schweinfurth, D.; Ehret, F.; Zalis, S.; Kvapilova, H.; Fiedler, J.; Zeng, Q.; Hartl, F.; Kaim, W. *Organometallics* **2014**, *33*, 4973−4985. (u) Le Goff, A.; Venec, D.; Le Roy, C.; Petillon, F. Y.; Schollhammer, P.; Talarmin, J. *Inorg. Chem.* **2014**, *53*, 2200−2210. (v) Leppin, J.; Foerster, C.; Heinze, K. *Inorg. Chem.* **2014**, *53*, 1039−1047. (w) McGuirk, C. M.; Stern, C. L.; Mirkin, C. A. *J. Am. Chem. Soc.* **2014**, *136*, 4689−4696. (x) Okuda, Y.; Ishiguro, Y.; Mori, S.; Nakajima, K.; Nishihara, Y. *Organometallics* **2014**, *33*, 1878−1889.

(y) Paretzki, A.; Bubrin, M.; Fiedler, J.; Zalis, S.; Kaim, W. *Chem.— Eur. J.* **2014**, *20*, 5414−5422. (z) Scheuermann, M. L.; Grice, K. A.; Ruppel, M. J.; Rosello-Merino, M.; Kaminsky, W.; Goldberg, K. I. *Dalton Trans.* **2014**, *43*, 12018−12025. (aa) Stephenson, C. J.; McInnis, J. P.; Chen, C.; Weberski, M. P.; Motta, A.; Delferro, M.; Marks, T. J. *ACS Catal.* **2014**, *4*, 999−1003. (ab) Zeng, M.; Li, L.; Herzon, S. B. *J. Am. Chem. Soc.* **2014**, *136*, 7058−7067. (ac) Yang, Y.; Liu, Z.; Cheng, R.; He, X.; Liu, B. *Organometallics* **2014**, *33*, 2599−2607.

(4) (a) Perry, M. C.; Cui, X.; Powell, M. T.; Hou, D.-R.; Reibenspies, J. H.; Burgess, K. *J. Am. Chem. Soc.* **2003**, *125*, 113−123. (b) Nanchen, S.; Pfaltz, A. *Chem.—Eur. J.* **2006**, *12*, 4550−4558. (c) Vicent, C.; Viciano, M.; Mas-Marzá, E.; Sanaú, M.; Peris, E. *Organometallics* **2006**, *25*, 3713−3720. (d) Wang, C.-Y.; Fu, C.-F.; Liu, Y.-H.; Peng, S.-M.; Liu, S.-T. *Inorg. Chem.* **2007**, *46*, 5779−5786. (e) Normand, A. T.; Cavell, K. J. *Eur. J. Inorg. Chem.* **2008**, 2781−2800. (f) Peng, H. M.; Webster, R. D.; Li, X. *Organometallics* **2008**, *27*, 4484−4493. (g) Dyson, G.; Frison, J.-C.; Whitwood, A. C.; Douthwaite, R. E. *Dalton Trans.* **2009**, 7141−7151. (h) Sun, J.-F.; Chen, F.; Dougan, B. A.; Xu, H.-J.; Cheng, Y.; Li, Y.-Z.; Chen, X.-T.; Xue, Z.-L. *J. Organomet. Chem.* **2009**, *694*, 2096−2105. (i) Jiménez, M. V.; Fernández-Tornos, J.; Pérez-Torrente, J. J.; Modrego, F. J.; Winterle, S.; Cunchillos, C.; Lahoz, F. J.; Oro, L. A. *Organometallics* **2011**, *30*, 5493−5508. (j) O, W. W. N.; Lough, A. J.; Morris, R. H. *Organometallics* **2013**, *32*, 3808− 3818. (k) Schumacher, A.; Bernasconi, M.; Pfaltz, A. *Angew. Chem., Int. Ed.* **2013**, *52*, 7422−7425.

(5) (a) Herrmann, W. A. *Angew. Chem., Int. Ed.* **2002**, *41*, 1290− 1309. (b) Hahn, F. E. *Angew. Chem., Int. Ed.* **2006**, *45*, 1348−1352. (c) Díez-González, S.; Nolan, S. P. *Coord. Chem. Rev.* **2007**, *251*, 874− 883. (d) Kühl, O. *Chem. Soc. Rev.* **2007**, *36*, 592−607. (e) Hahn, F. E.; Jahnke, M. C. *Angew. Chem., Int. Ed.* **2008**, *47*, 3122−3172. (f) Díez- González, S.; Marion, N.; Nolan, S. P. *Chem. Rev.* **2009**, *109*, 3612− 3676. (g) Jacobsen, H.; Correa, A.; Poater, A.; Costabile, C.; Cavallo, L. *Coord. Chem. Rev.* **2009**, *253*, 687−703. (h) Dröge, T.; Glorius, F. *Angew. Chem., Int. Ed.* **2010**, *49*, 6940−6952. (i) Glorius, F.; Bellemin- Laponnaz, S. In *N-Heterocyclic Carbenes in Transition Metal Catalysis;* Springer: Berlin, Germany, 2007. (j) Cazin, C. S. J. In *Heterocyclic Carbenes in Transition Metal Catalysis and Organocatalysis;* Springer: Berlin, Germany, 2011;. (k) Díez-González, S. In *N-Heterocyclic Carbenes: From Laboratory Curiosities to Efficient Synthetic Tools;* Royal Society of Chemistry: Cambridge, U.K., 2011.

(6) Recent research results from our group on transition metal NHC complexes and their multidentate variants: (a) Gigler, P.; Bechlars, B.; Herrmann, W. A.; Kühn, F. E. *J. Am. Chem. Soc.* **2011**, *133*, 1589− 1596. (b) Raba, A.; Cokoja, M.; Ewald, S.; Riener, K.; Herdtweck, E.; Pöthig, A.; Herrmann, W. A.; Kühn, F. E. *Organometallics* **2012**, *31*, 2793−2800. (c) Schaper, L.-A.; Öfele, K.; Kadyrov, R.; Bechlars, B.; Drees, M.; Cokoja, M.; Herrmann, W. A.; Kühn, F. E. *Chem. Commun.* **2012**, *48*, 3857−3859. (d) Jantke, D.; Cokoja, M.; Drees, M.; Herrmann, W. A.; Kühn, F. E. *ChemCatChem* **2013**, *5*, 3241−3248. (e) Jantke, D.; Cokoja, M.; Pöthig, A.; Herrmann, W. A.; Kühn, F. E. *Organometallics* **2013**, *32*, 741−744. (f) Reindl, S. A.; Pöthig, A.; Drees, M.; Bechlars, B.; Herdtweck, E.; Herrmann, W. A.; Kühn, F. E. *Organometallics* **2013**, *32*, 4082−4091. (g) Schaper, L.-A.; Graser, L.; Wei, X.; Zhong, R.; Öfele, K.; Pöthig, A.; Cokoja, M.; Bechlars, B.; Herrmann, W. A.; Kühn, F. E. *Inorg. Chem.* **2013**, *52*, 6142−6152. (h) Schaper, L.-A.; Wei, X.; Altmann, P. J.; Öfele, K.; Pöthig, A.; Drees, M.; Mink, J.; Herdtweck, E.; Bechlars, B.; Herrmann, W. A.; Kühn, F. E. *Inorg. Chem.* **2013**, *52*, 7031−7044. (i) Schaper, L.-A.; Wei, X.; Hock, S. J.; Pöthig, A.; Öfele, K.; Cokoja, M.; Herrmann, W. A.; Kühn, F. E. *Organometallics* **2013**, *32*, 3376−3384. (j) Kück, J. W.; Raba, A.; Markovits, I. I. E.; Cokoja, M.; Kühn, F. E. *ChemCatChem* **2014**, *6*, 1882−1886.

(7) Raba, A.; Anneser, M. R.; Jantke, D.; Cokoja, M.; Herrmann, W. A.; Kühn, F. E. *Tetrahedron Lett.* **2013**, *54*, 3384−3387.

(8) (a) Chen, J. C. C.; Lin, I. J. B. *Organometallics* **2000**, *19*, 5113− 5121. (b) Lee, K.-M.; Chen, J. C. C.; Lin, I. J. B. *J. Organomet. Chem.* **2001**, *617−618*, 364−375.

(9) Basson, S. S.; Leipoldt, J. G.; Purcell, W.; Schoeman, J. B. *Inorg. Chim. Acta* **1990**, *173*, 155−158.

(10) Fagnou, K.; Lautens, M. *Angew. Chem., Int. Ed.* **2002**, *41*, 26−47.

(11) (a) Hitchcock, P. B.; Lappert, M. F.; Terreros, P. *J. Organomet. Chem.* **1982**, *239*, C26−C30. (b) Danopoulos, A. A.; Winston, S.; Hursthouse, M. B. *J. Chem. Soc., Dalton Trans.* **2002**, 3090−3091. (c) Crudden, C. M.; Allen, D. P. *Coord. Chem. Rev.* **2004**, *248*, 2247−2273. (d) Sinha, A.; Wahidur, R. S. M.; Sarkar, M.; Saha, B.; Daw, P.; Bera, J. K. *Inorg. Chem.* **2009**, *48*, 11114−11122.

(12) Stylianides, N.; Danopoulos, A. A.; Tsoureas, N. *J. Organomet. Chem.* **2005**, *690*, 5948−5958.

(13) Mas-Marzá, E.; Sanaú, M.; Peris, E. *Inorg. Chem.* **2005**, *44*, 9961−9967.

(14) Scherg, T.; Schneider, S. K.; Frey, G. D.; Schwarz, J.; Herdtweck, E.; Herrmann, W. A. *Synlett* **2006**, 2894−2907.

(15) (a) Gnanamgari, D.; Moores, A.; Rajaseelan, E.; Crabtree, R. H. *Organometallics* **2007**, *26*, 1226−1230. (b) Türkmen, H.; Pape, T.; Hahn, F. E.; Çetinkaya, B. *Organometallics* **2008**, *27*, 571−575. (c) Türkmen, H.; Pape, T.; Hahn, F. E.; Çetinkaya, B. *Eur. J. Inorg. Chem.* **2008**, 5418−5423. (d) Kownacki, I.; Kubicki, M.; Szubert, K.; Marciniec, B. *J. Organomet. Chem.* **2008**, *693*, 321−328. (e) Ogle, J. W.; Miller, S. A. *Chem. Commun.* **2009**, 5728−5730. (f) Zinner, S. C.; Rentzsch, C. F.; Herdtweck, E.; Herrmann, W. A.; Kühn, F. E. *Dalton Trans.* **2009**, 7055−7062. (g) Diez, C.; Nagel, U. *Appl. Organomet. Chem.* **2010**, *24*, 509−516. (h) Binobaid, A.; Iglesias, M.; Beetstra, D.; Dervisi, A.; Fallis, I.; Cavell, K. J. *Eur. J. Inorg. Chem.* **2010**, 5426−5431. (i) Gong, X.; Zhang, H.; Li, X. *Tetrahedron Lett.* **2011**, *52*, 5596−5600. (j) Newman, P. D.; Cavell, K. J.; Hallett, A. J.; Kariuki, B. M. *Dalton Trans.* **2011**, *40*, 8807−8813. (k) Ashley, J. M.; Farnaby, J. H.; Hazari, N.; Kim, K. E.; Luzik, E. D., Jr; Meehan, R. E.; Meyer, E. B.; Schley, N. D.; Schmeier, T. J.; Tailor, A. N. *Inorg. Chim. Acta* **2012**, *380*, 399−410. (l) Mena, I.; Jaseer, E. A.; Casado, M. A.; García-Orduña, P.; Lahoz, F. J.; Oro, L. A. *Chem.—Eur. J.* **2013**, *19*, 5665−5675. (m) Gülcemal, S.; Gökçe, A. G.; Çetinkaya, B. *Inorg. Chem.* **2013**, *52*, 10601−10609. (n) Gülcemal, S.; Gökçe, A. G.; Çetinkaya, B. *Dalton Trans.* **2013**, *42*, 7305−7311. (o) Andersson, P. G. In *Iridium Catalysis*; Springer: Berlin, Germany, 2011.

(16) Ouali, A.; Majoral, J.-P.; Caminade, A.-M.; Taillefer, M. *ChemCatChem* **2009**, *1*, 504−509.

(17) (a) Yamagata, T.; Tadaoka, H.; Nagata, M.; Hirao, T.; Kataoka, Y.; Ratovelomanana-Vidal, V.; Genet, J. P.; Mashima, K. *Organometallics* **2006**, *25*, 2505−2513. (b) Núñez-Rico, J. L.; Fernández-Pérez, H.; Benet-Buchholz, J.; Vidal-Ferran, A. *Organometallics* **2010**, *29*, 6627−6631. (c) Passarelli, V.; Pérez-Torrente, J. J.; Oro, L. A. *Inorg. Chem.* **2014**, *53*, 972−980.

(18) Recent examples of iridium(I) NHC CO halide complexes: (a) Hildebrandt, B.; Raub, S.; Frank, W.; Ganter, C. *Chem.—Eur. J.* **2012**, *18*, 6670−6678. (b) Arumugam, K.; Varnado, C. D.; Sproules, S.; Lynch, V. M.; Bielawski, C. W. *Chem.—Eur. J.* **2013**, *19*, 10866−10875. (c) Buhl, H.; Ganter, C. *Chem. Commun.* **2013**, *49*, 5417−5419. (d) Karthik, V.; Bhat, I. A.; Anantharaman, G. *Organometallics* **2013**, *32*, 7006−7013. (e) Valdés, H.; Poyatos, M.; Peris, E. *Organometallics* **2013**, *33*, 394−401. (f) Valdés, H.; Poyatos, M.; Peris, E. *Organometallics* **2013**, *32*, 6445−6451. (g) van Weerdenburg, B. J. A.; Gloggler, S.; Eshuis, N.; Engwerda, A. H. J.; Smits, J. M. M.; de Gelder, R.; Appelt, S.; Wymenga, S. S.; Tessari, M.; Feiters, M. C.; Blumich, B.; Rutjes, F. P. J. T. *Chem. Commun.* **2013**, *49*, 7388−7390.

(19) Cowley, M. J.; Adams, R. W.; Atkinson, K. D.; Cockett, M. C. R.; Duckett, S. B.; Green, G. G. R.; Lohman, J. A. B.; Kerssebaum, R.; Kilgour, D.; Mewis, R. E. *J. Am. Chem. Soc.* **2011**, *133*, 6134−6137.

(20) Tolman, C. A. *J. Am. Chem. Soc.* **1970**, *92*, 2956−2965.

(21) Frazier, J. F.; Merola, J. S. *Polyhedron* **1992**, *11*, 2917−2927.

(22) (a) Powell, M. T.; Hou, D.-R.; Perry, M. C.; Cui, X.; Burgess, K. *J. Am. Chem. Soc.* **2001**, *123*, 8878−8879. (b) Jeon, S.-J.; Waymouth, R. M. *Dalton Trans.* **2008**, 437−439. (c) Wheatley, J. E.; Ohlin, C. A.; Chaplin, A. B. *Chem. Commun.* **2014**, *50*, 685−687.

(23) Vazquez-Serrano, L. D.; Owens, B. T.; Buriak, J. M. *Chem. Commun.* **2002**, 2518−2519.

(24) Nelson, D. J.; Nolan, S. P. *Chem. Soc. Rev.* **2013**, *42*, 6723−6753.

(25) (a) Tang, C. Y.; Smith, W.; Vidovic, D.; Thompson, A. L.; Chaplin, A. B.; Aldridge, S. *Organometallics* **2009**, *28*, 3059−3066. (b) Torres, O.; Martín, M.; Sola, E. *Organometallics* **2009**, *28*, 863−870. (c) Dobereiner, G. E.; Nova, A.; Schley, N. D.; Hazari, N.; Miller, S. J.; Eisenstein, O.; Crabtree, R. H. *J. Am. Chem. Soc.* **2011**, *133*, 7547−7562. (d) Schultz, K. M.; Goldberg, K. I.; Gusev, D. G.; Heinekey, D. M. *Organometallics* **2011**, *30*, 1429−1437.

(26) (a) Rahaman, S. M. W.; Dinda, S.; Sinha, A.; Bera, J. K. *Organometallics* **2013**, *32*, 192−201. (b) Gründemann, S.; Kovacevic, A.; Albrecht, M.; Faller, J. W.; Crabtree, R. H. *J. Am. Chem. Soc.* **2002**, *124*, 10473−10481. (c) Xiao, X.-Q.; Jin, G.-X. *J. Organomet. Chem.* **2008**, *693*, 3363−3368. (d) Gnanamgari, D.; Sauer, E. L. O.; Schley, N. D.; Butler, C.; Incarvito, C. D.; Crabtree, R. H. *Organometallics* **2009**, *28*, 321−325. (e) Kessler, F.; Costa, R. D.; Di Censo, D.; Scopelliti, R.; Orti, E.; Bolink, H. J.; Meier, S.; Sarfert, W.; Grätzel, M.; Nazeeruddin, M. K.; Baranoff, E. *Dalton Trans.* **2012**, *41*, 180−191.

(27) Armarego, W. L. F.; Chai, C. L. L. In *Purification of Laboratory Chemicals*; Butterworth-Heinemann: Oxford, U.K., 2003.

(28) Frisch, M. J.; Trucks, G. W.; Schlegel, H. B.; Scuseria, G. E.; Robb, M. A.; Cheeseman, J. R.; Scalmani, G.; Barone, V.; Mennucci, B.; Petersson, G. A.; Nakatsuji, H.; Caricato, M.; Li, X.; Hratchian, H. P.; Izmaylov, A. F.; Bloino, J.; Zheng, G.; Sonnenberg, J. L.; Hada, M.; Ehara, M.; Toyota, K.; Fukuda, R.; Hasegawa, J.; Ishida, M.; Nakajima, T.; Honda, Y.; Kitao, O.; Nakai, H.; Vreven, T.; Montgomery, J. A., Jr.; Peralta, J. E.; Ogliaro, F.; Bearpark, M.; Heyd, J. J.; Brothers, E.; Kudin, K. N.; Staroverov, V. N.; Kobayashi, R.; Normand, J.; Raghavachari, K.; Rendell, A.; Burant, J. C.; Iyengar, S. S.; Tomasi, J.; Cossi, M.; Rega, N.; Millam, N. J.; Klene, M.; Knox, J. E.; Cross, J. B.; Bakken, V.; Adamo, C.; Jaramillo, J.; Gomperts, R.; Stratmann, R. E.; Yazyev, O.; Austin, A. J.; Cammi, R.; Pomelli, C.; Ochterski, J. W.; Martin, R. L.; Morokuma, K.; Zakrzewski, V. G.; Voth, G. A.; Salvador, P.; Dannenberg, J. J.; Dapprich, S.; Daniels, A. D.; Farkas, Ö.; Foresman, J. B.; Ortiz, J. V.; Cioslowski, J.; Fox, D. J. *Gaussian 09*, Revision D.01; Gaussian Inc., Wallingford: CT, 2009.

(29) (a) Vosko, S. H.; Wilk, L.; Nusair, M. *Can. J. Phys.* **1980**, *58*, 1200−1211. (b) Lee, C.; Yang, W.; Parr, R. G. *Phys. Rev. B* **1988**, *37*, 785−789. (c) Becke, A. D. *J. Chem. Phys.* **1993**, *98*, 5648−5652. (d) Stephens, P. J.; Devlin, F. J.; Chabalowski, C. F.; Frisch, M. J. *J. Phys. Chem.* **1994**, *98*, 11623−11627.

(30) (a) McLean, A. D.; Chandler, G. S. *J. Chem. Phys.* **1980**, *72*, 5639−5648. (b) Krishnan, R.; Binkley, J. S.; Seeger, R.; Pople, J. A. *J. Chem. Phys.* **1980**, *72*, 650−654. (c) Binning, R. C.; Curtiss, L. A. *J. Comput. Chem.* **1990**, *11*, 1206−1216. (d) McGrath, M. P.; Radom, L. *J. Chem. Phys.* **1991**, *94*, 511−516. (e) Curtiss, L. A.; McGrath, M. P.; Blaudeau, J. P.; Davis, N. E.; Binning, R. C.; Radom, L. *J. Chem. Phys.* **1995**, *103*, 6104−6113.

(31) Stuttgart RSC 1997 ECP basis set was obtained from the EMSL Basis Set Library, version October 15, 2008; Schuchardt, K. L.; Didier, B. T.; Elsethagen, T.; Sun, L.; Gurumoorthi, V.; Chase, J.; Li, J.; Windus, T. L. *J. Chem. Inf. Model.* **2007**, *47*, 1045−1052.

(32) (a) Cossi, M.; Barone, V.; Cammi, R.; Tomasi, J. *Chem. Phys. Lett.* **1996**, *255*, 327−335. (b) Tomasi, J.; Mennucci, B.; Cammi, R. *Chem. Rev.* **2005**, *105*, 2999−3094.